Supplementary Figure 1

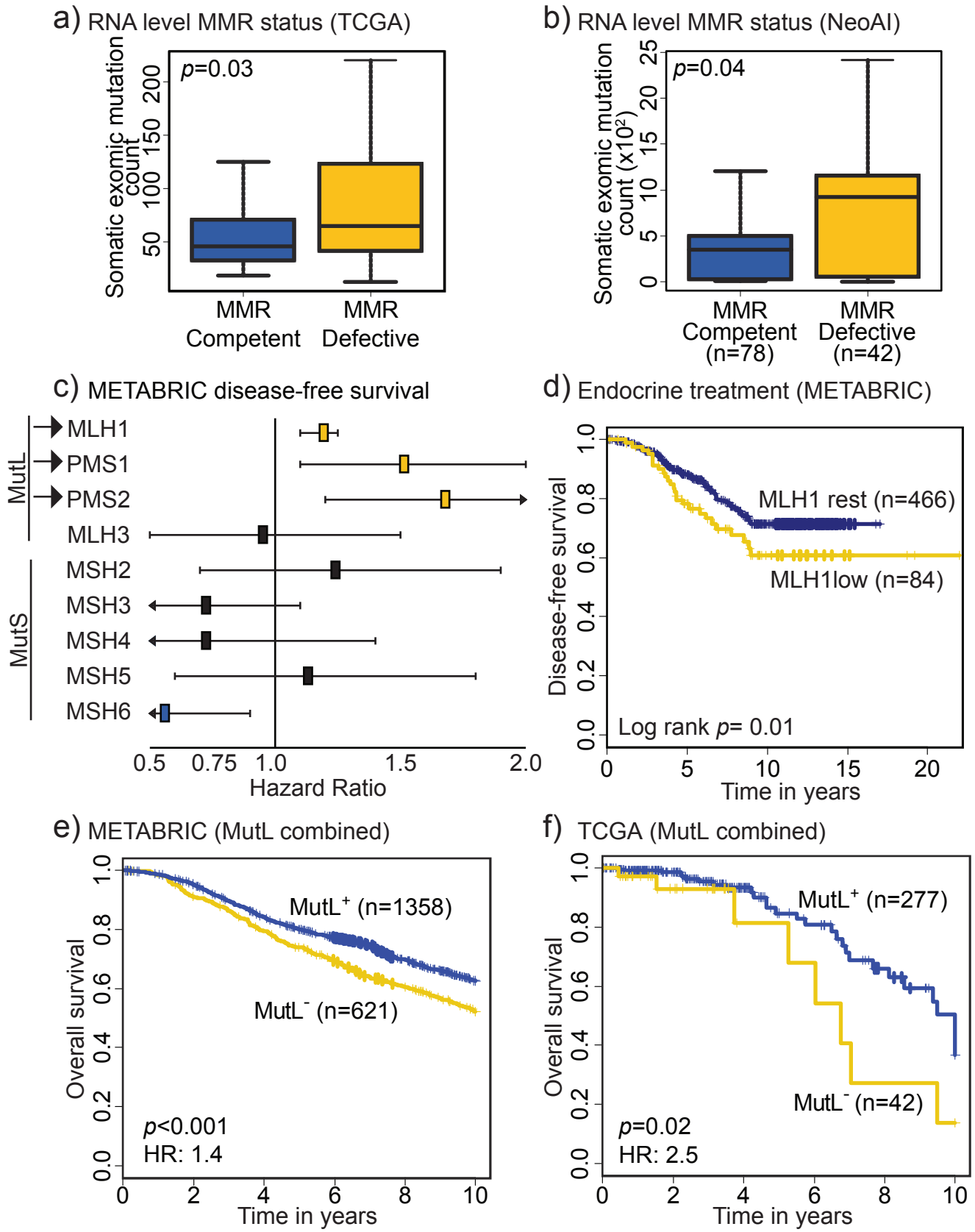

Supplementary Figure 2

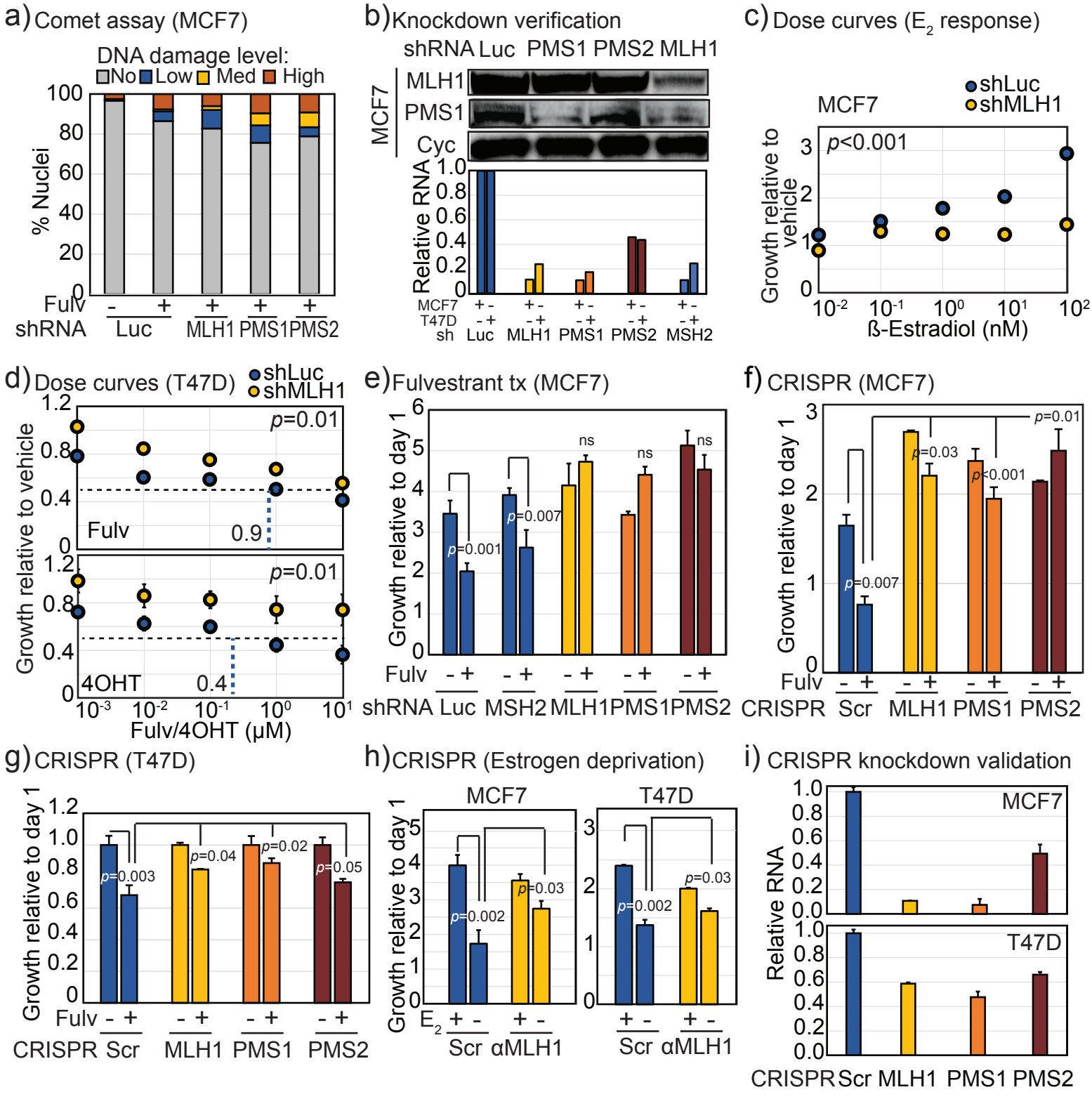

Supplementary Figure 3

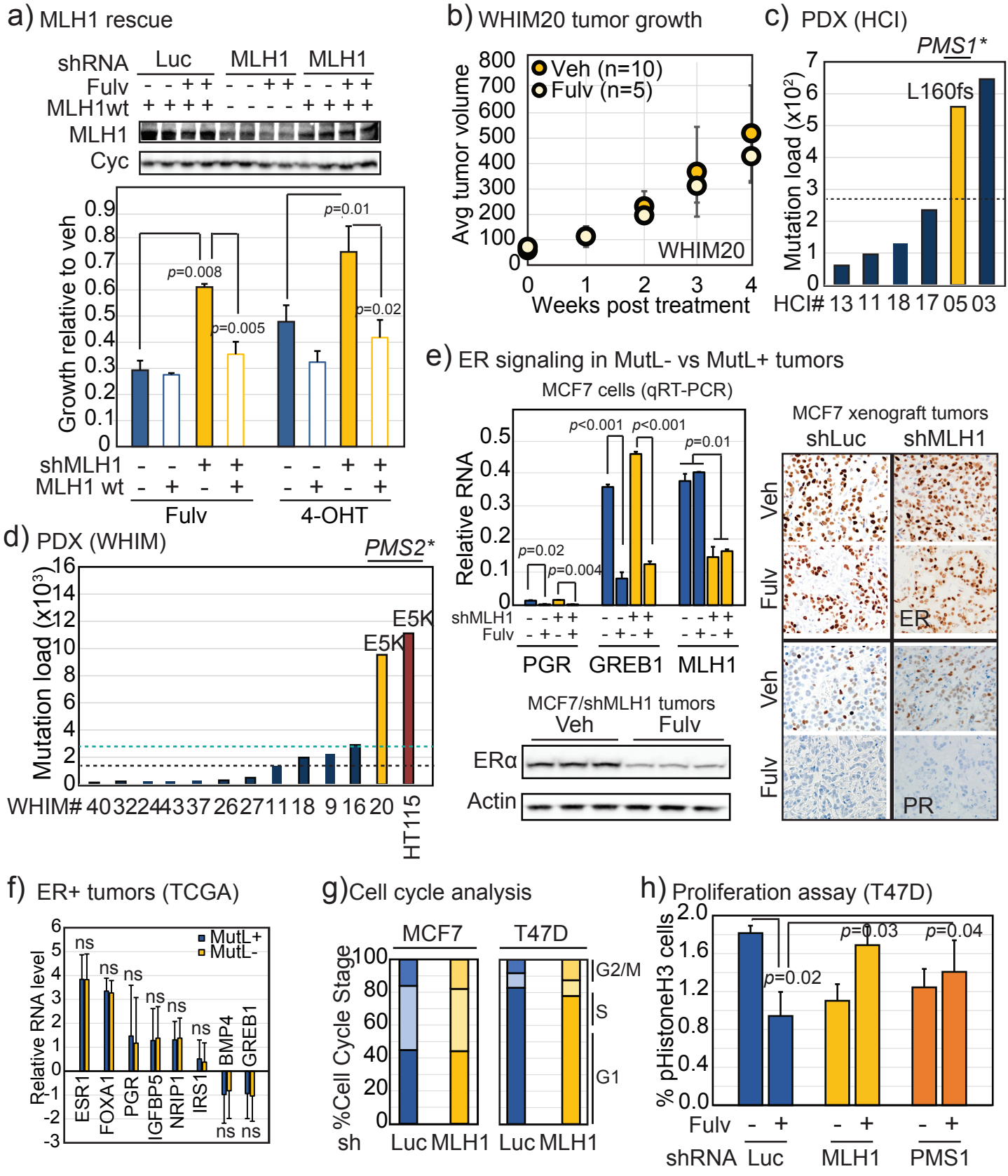

Supplementary Figure 4

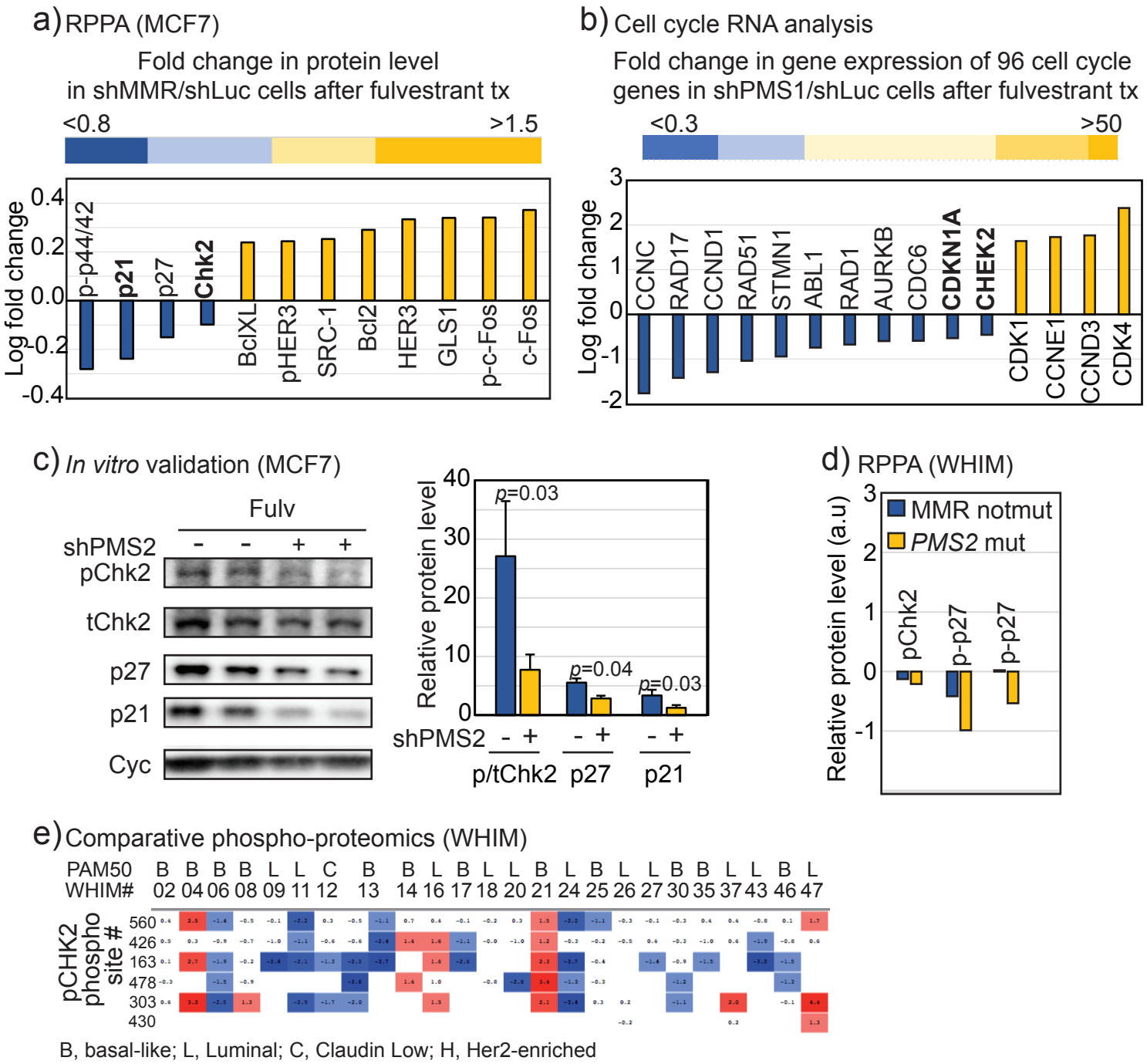

Supplementary Figure 5

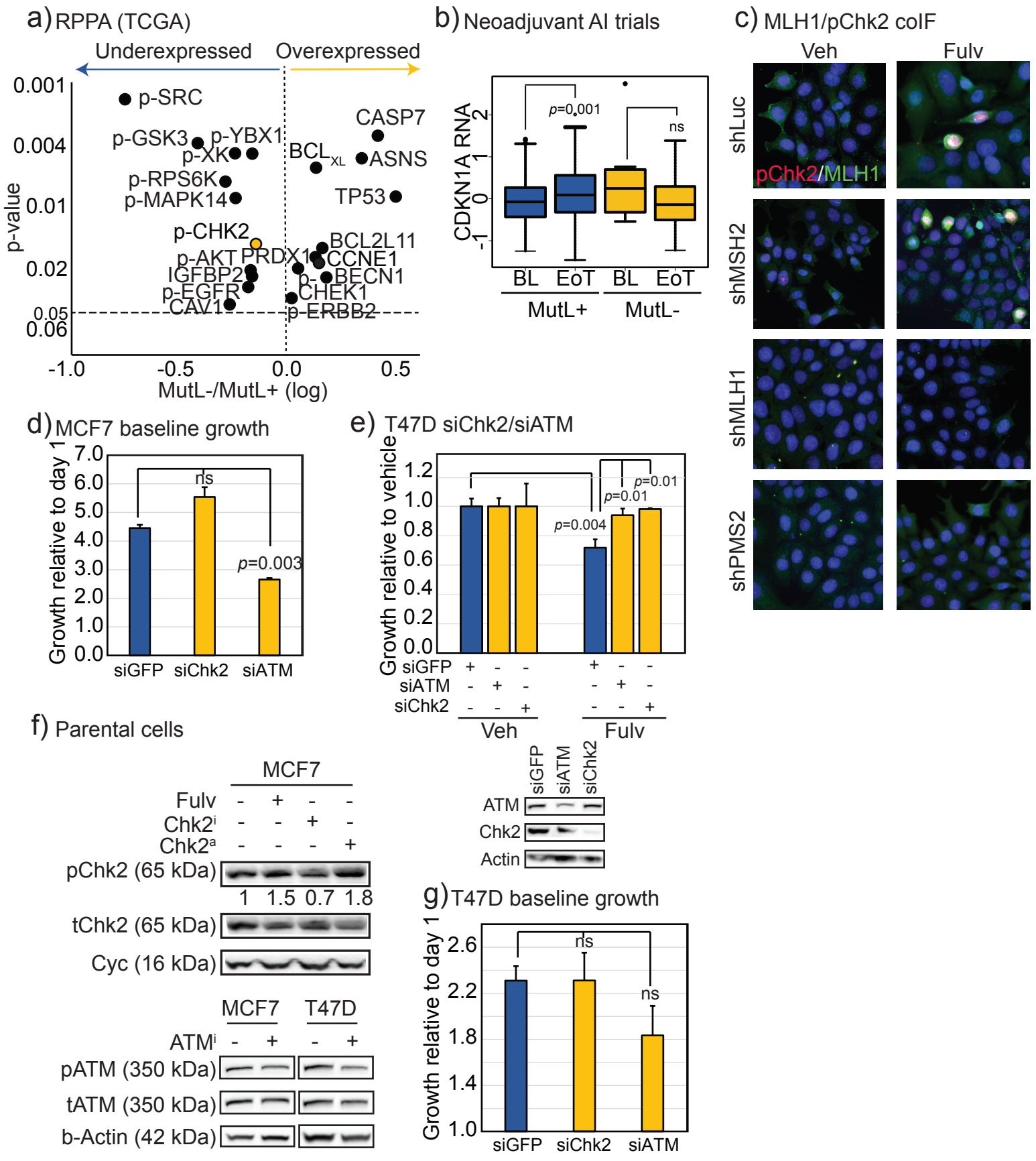

Supplementary Figure 7

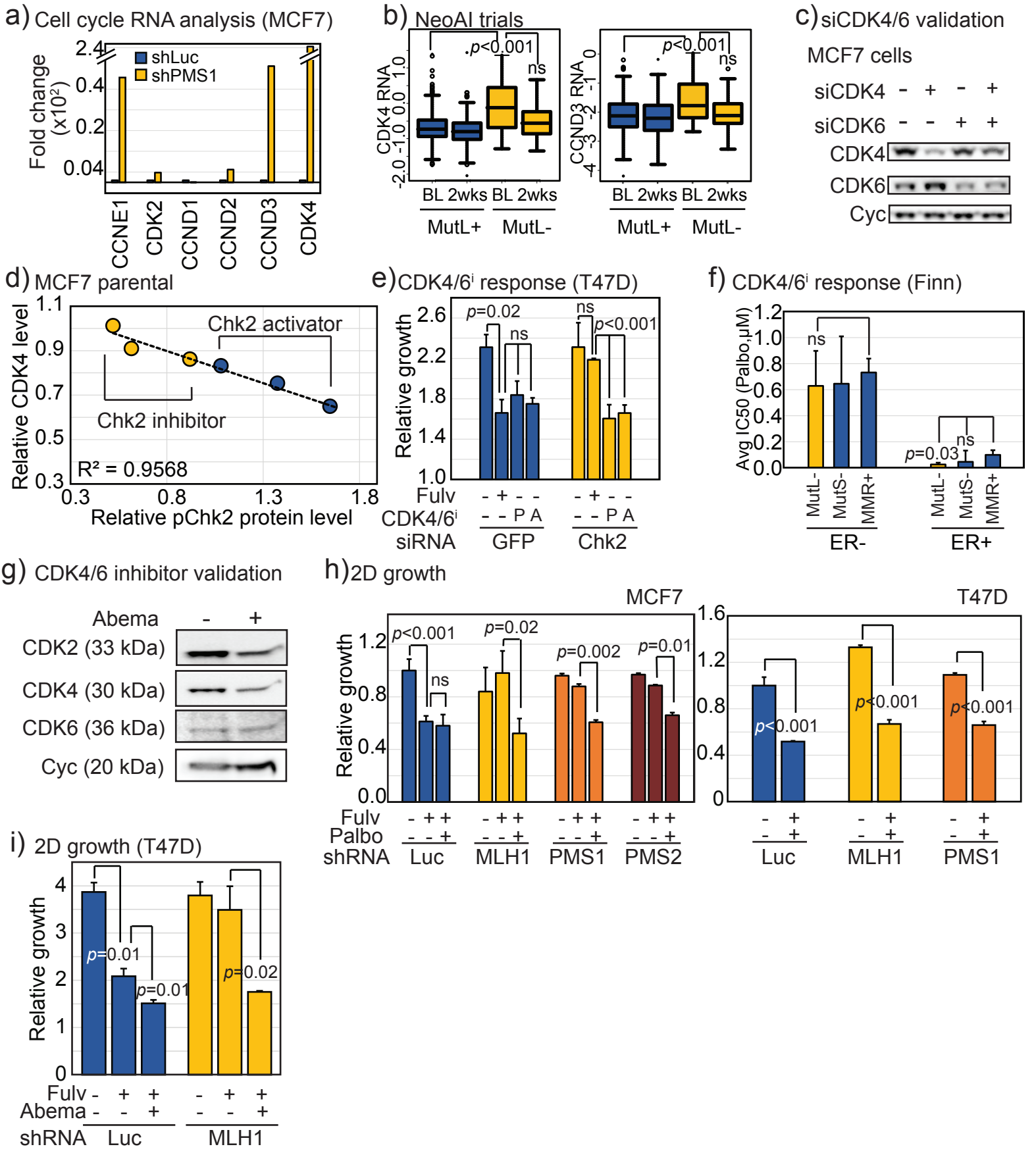

Supplementary Figure 6

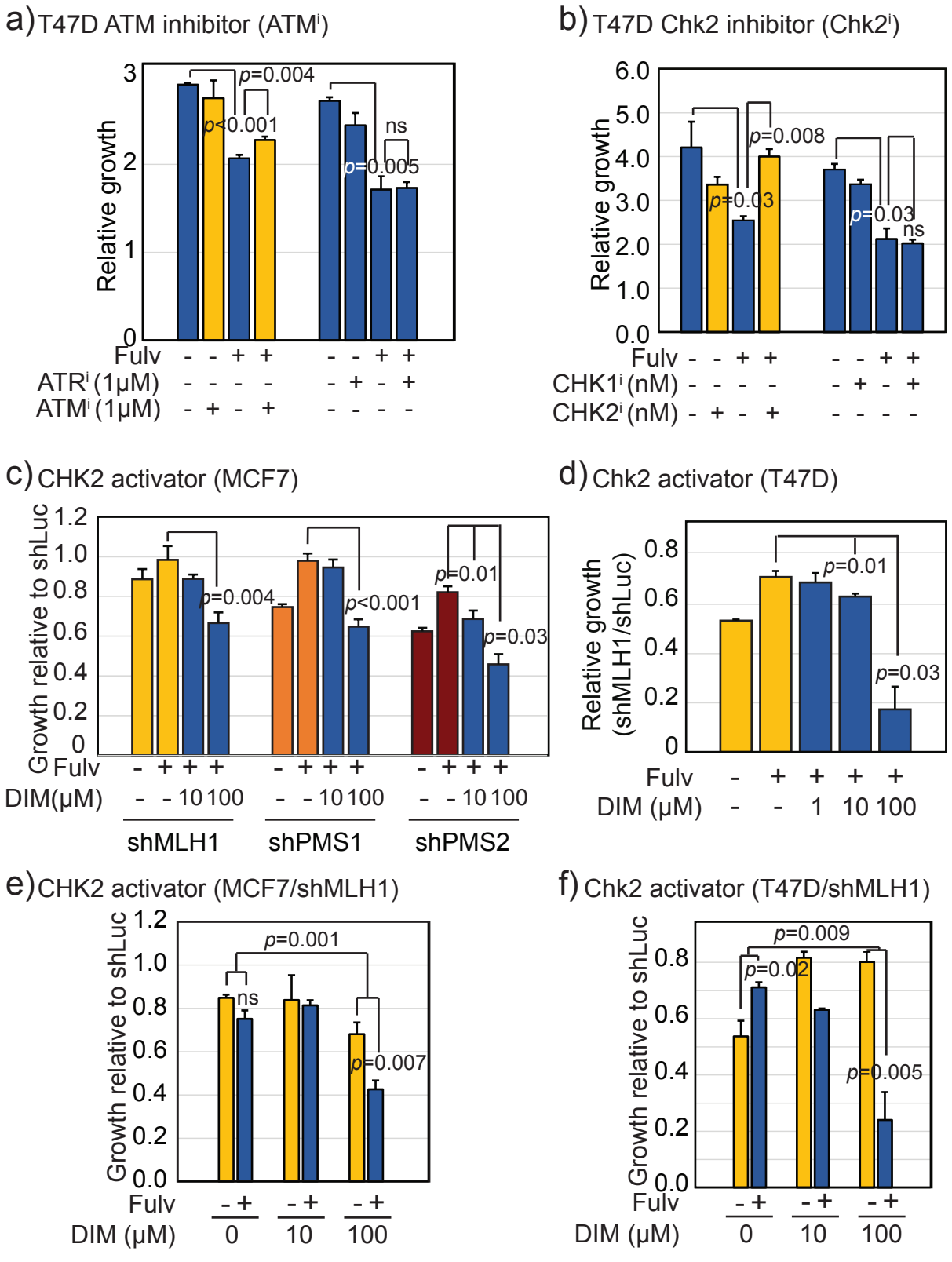

Supplementary Figure Legends

Supplementary Figure 1 Mismatch repair dysregulation associates with high mutation load and poor clinical outcome in patients with ER^+ breast cancer.

a+b) ER^+ tumors with low mRNA levels (<mean-1.5xStDevn) of pathway-unique MMR genes from TCGA (**a**) and NeoAI (**b**) datasets have increased overall exomic mutation load compared to tumors without. Kruskal Wallis test determined *p*-values. **c**) Forest plot demonstrating that ER^+ tumors with low MutL (MLH1, MLH3, PMS1 and/or PMS2) gene RNA in METABRIC associate selectively with poor disease-free survival. Log rank test was used to determine significance. Benjamini-Hochberg correction applied for multiple comparisons. **d-f**) Kaplan-Meier survival curves of patients having low RNA levels of MLH1 (**d**), or mutation (**e**) and/or low RNA levels (**e+f**) of and MutL gene ($MutL^-$) relative to all other endocrine therapy treated ER^+ tumors in METABRIC (**d+e**) ($MutL^+$) or to all other patients with luminal tumors from TCGA (**f**) ($MutL^+$). Differences in survival were determined using log rank test. Accompanying information presented in **Fig 1.**

Supplementary Figure 2 MutL complex disruption in ER^+ breast cancer cells induces endocrine therapy resistance.

a+b) Validation of MutL and MSH2 disruption in MCF7 cells by assaying for increased DNA damage as a biological phenotype (Comet assay (**a**)), and for protein and RNA levels using Western blots and qRT-PCR respectively (**b**). Low baseline levels of PMS2 and lack of appropriate antibodies precluded Western blot analysis of protein levels. Quantification performed using CaspLab (**a**) and Image Lab analysis software (**b**). Pearson's chi square comparing proportion of damaged nuclei in each shMutL cell line relative to control (shLuc) treated with fulvestrant determined *p*-value<0.01 when comparing shLuc treated with fulvestrant *vs* any of the other groups (**a**). **c+d**) Dose curves demonstrating increased growth of MCF7 (**c**) and T47D (**d**)

cells stably expressing shRNA against MLH1 (shMLH1) in response to increasing doses of beta-estradiol (**c**), 4-hydroxy tamoxifen (4-OHT, **d-bottom**) and fulvestrant (Fulv, **d-top**) relative to cells expressing shRNA against control (Luc, Luciferase). *p*-value describes significance of difference between slopes. **e-h**) Bar graphs indicating fold change in growth after fulvestrant treatment (**e-g**) or estrogen deprivation (**h**) of MCF7 (**e-f+h-left**) and T47D (**g+h-right**) cells stably expressing either shRNA (**e**) or CRISPR (**f-h**) against MutL genes, *MSH2*, *MLH1*, *PMS1* or *PMS2* as specified, and cells expressing shRNA against luciferase or scrambled CRISPR controls respectively. **i**) Bar graph indicating fold change in RNA levels of MutL genes in MCF7 (top) and T47D (bottom) cells transiently transfected with CRISPR constructs against them. Supports data presented in **Fig 2**. Student's t-test generated *p*-values. Columns=mean, error bars=standard deviation, except for (**a**).

Supplementary Figure 3 Spontaneously MutL-deficient ER^+ breast cancer cells are endocrine therapy resistant.

a) 2D growth of MCF7 cells stably expressing shRNA against Luciferase (shLuc) or MLH1 (shMLH1), and overexpressing sh-resistant MLH1 cDNA, after either tamoxifen (4-OHT) or fulvestrant (Fulv) treatment. **b**) Tumor growth curves of the WHIM20 PDX treated with either vehicle or fulvestrant indicating lack of sensitivity of WHIM20 to the endocrine intervention. **c+d**) Index plots showing exomic mutation load across all ER^+ WHIM (**d**) and HCI PDX tumors (**c**). A hypermutator colorectal cancer cell line, HT115, is included for comparison as it shares an identical mutation in a MutL gene, *PMS2*, with WHIM20. **e**) qRT-PCR analysis of ER target gene RNA levels (top left), Western blot assay for protein levels of ER (bottom left), and immunohistochemistry for ER and PR protein levels (right) in MCF7 shLuc and shMLH1 cells *in vitro*, and *in vivo*, demonstrating comparable baseline levels and significant inhibition of ER signaling in response to fulvestrant (Fulv) treatment. **f**) Analysis of RNA levels of ER target genes

in human ER^+ tumors that are either $MutL^-$ (defined as in **Fig 1**) or $MutL^+$. **g**) Column graph representing proportion of cells in G1, S and G2/M stages of the cell cycle 48 hours after plating MCF7 and T47D shLuc and shMLH1 cells in full serum growth media. **h**) Bar graph representing total percentage of mitotic cells in T47D cells stably expressing shRNA against luciferase (shLuc), MLH1 (shMLH1) or PMS1 (shPMS1) in the presence or absence of fulvestrant treatment as assayed by immunofluorescence for pHistoneH3. Error bars describe standard deviation and Student's t-test determined *p*-values. Supports data presented in **Fig 2**.

Supplementary Figure 4 MutL deficient cells induce endocrine therapy resistance *via* Chk2.

a+b) Bar graphs quantifying most significantly dysregulated proteins as assayed by RPPA (**a**) and cell cycle genes assayed by qRT-PCR (**b**) in MCF7 shMLH1, shPMS1 or shPMS2 (as indicated) cells relative to shLuc after administration of fulvestrant treatment for 48 hours. *P*-values were determined by Student's t-test and FDR adjusted using Benjamini-Hochberg. Supports data presented in **Fig 3a**. **c**) Western blots demonstrating decreased protein levels of pChk2, p21 and p27 in PMS2-silenced MCF7 cells after fulvestrant treatment with accompanying quantification (Image Lab software). Four independent samples per quantified Western blot. Supports data presented in **Fig 3b**. Student's t-test generated *p*-values. **d**) Bar graph depicting protein level changes in pChk2 and p-p27 based on RPPA in *PMS2* mutant WHIM20 PDX relative to 9 other ER^+ PDX tumors (all tumors grown in estrogen deprived conditions). Two independent phosphorylation sites for p27 (T157 and T198) were validated, both annotated as p-p27. RPPA array did not include antibodies against p21. **e**) Heat map of Chk2 phosphorylation based on mass-spectrometry phospho-proteomics across all WHIM PDX lines after estrogen deprivation (low to high, blue to red). Supports WHIM16 and WHIM20 Western blot validation in **Fig 3d**. For all graphs, columns represent the mean and error bars describe standard deviation.

Supplementary Figure 5 Chk2 activation is required for response to endocrine therapy in ER^+ breast cancer cells.

a) Proteins that are significantly (p<0.05) overexpressed or underexpressed in an unbiased comparison of $MutL^-$ and $MutL^+$ ER^+ tumors from TCGA (as defined in **Fig S1f**). Proteins highlighted in yellow were identified in empirical assays. Supports data presented in **Fig 3**. **b**) Box plot denoting changes in CDKN1A (p21) RNA levels after 2-4 weeks of endocrine treatment (EoT) relative to baseline levels at diagnosis (BL) in $MutL^-$ *vs* $MutL^+$ ER^+ tumors from the NeoAI datasets (as defined in **Fig 1e**). Supports data presented in **Fig 3**. **c**) Co-IF for MLH1 and pChk2 in MCF7 $MutL^+$ (shLuc, shMSH2) and $MutL^-$ (shMLH1, shPMS2) cells with either vehicle or fulvestrant treatment. DAPI as nuclear stain. Magnification: 20x. Supports data presented in **Fig 4a+b**. **d+e, g**) Bar graphs representing changes in growth of MCF7 (**d**) and T47D (**e+g**) cells treated with siGFP, siATM or siChk2 at baseline and after fulvestrant treatment with accompanying Western blot validation of knockdown in T47D cells (**e**). Supports data presented in **Fig 4c+d**. **f**) Western blot validation of Chk2 and ATM inactivation in MCF7 cells treated with Chk2 inhibitors or activators, and ATM inhibitor. Supports data presented in **Fig 4e+f+S6**. Student's t-test generated *p*-values for all analyses except (**b**) where Wilcoxon Rank Sum test was used. Columns represent mean and error bars the standard deviation for all bar graphs.

Supplementary Figure 6 Chk2 activation is sufficient to sensitize MutL proficient ER^+ breast cancer cells to endocrine therapy.

Bar graphs demonstrate that ATM (**a**) and Chk2 (**b**) inhibition using pharmacological inhibitors in T47D parental cells induces resistance to fulvestrant, and Chk2 activation using increasing doses of the natural chemopreventive agent, 3', 3'-diindolyl methane (DIM) in $MutL^-$ MCF7 (**c+e**) and shMLH1 T47D (**d+f**) cells resensitizes them to endocrine therapy, represented by fulvestrant (Fulv) treatment. Growth represented relative to $MutL^+$ shLuc to demonstrate increased sensitivity

of MutL$^-$ cells. Growth in response to DIM alone represented in **e+f**. Student's t-test generated all *p*-values. Error bars represent standard deviation. Supports data presented in **Fig 4**.

Supplementary Figure 7 MutL deficient ER$^+$ breast cancer cells can be sensitized to endocrine treatment by combinatorial administration of CDK4/6 inhibitors.

a) Bar graphs indicating genes whose expression increased most significantly in MutL$^-$ (shPMS1) *vs* MutL$^+$ (shLuc) cells after fulvestrant treatment. Interpretation of these differences in gene expression must be made within the context of differential proliferative response to endocrine treatment between MutL- and MutL+ breast cancer cells **b)** Boxplots depicting change in RNA levels of CDK4 and CCND3 in biopsies taken at diagnosis (BL, baseline) and after 2-4 weeks of endocrine treatment (2wks) from MutL$^-$ and MutL$^+$ ER$^+$ tumors in the NeoAI dataset (defined as in **Fig 1e**). **c**) Regression analysis determining inverse correlation between protein levels of pChk2 and CDK4 in MCF7 cells treated with Chk2 inhibitor or DIM (Chk2 activator), as assayed by Western blot (representative Western blot in **Fig S5f**). **d+g**) Western blots validating CDK4 and CDK6 inhibition with respective siRNAs (**d**) and CDK2, 4 and 6 inhibition in MCF7 cells after treatment with CDK4/6 inhibitor, Abemaciclib (**g**). **e+f+h+i**) Bar graphs depicting decreased growth of T47D/siChk2 cells in response to either palbociclib (P) or abemaciclib (A) (**e**), increased sensitivity to palbociclib of MutL$^-$ ER$^+$ breast cancer cell lines from analysis of data from the Finn dataset (**f**), and of MutL$^-$ MCF7 (**h-**left) and T47D (**h-**right, **i**) cells treated with combination of fulvestrant and CDK4/6 inhibitor (Palbociclib, **h** and Abemaciclib, **i**). Student's t-test generated all *p*-values, except for (**b**) where Wilcoxon Rank Sum test was used. Error bars represent standard deviation, except in (**b**) where error bars = standard error. Supports data presented in **Figs 5+6**.